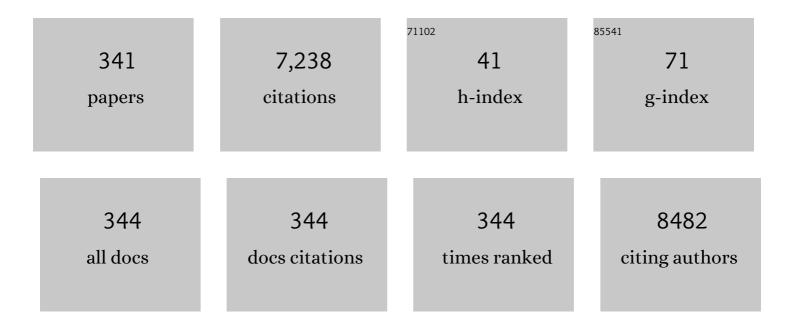
List of Publications by Year in descending order

Source: https://exaly.com/author-pdf/2921382/publications.pdf Version: 2024-02-01



TILDEL CHEN

| # | Article | IF | CITATIONS |
|----|---|-----|-----------|
| 1 | Epilepsy detection with artificial neural network based on as-fabricated neuromorphic chip platform. AIP Advances, 2022, 12, 035106. | 1.3 | 3 |
| 2 | Transparent electronic and photoelectric synaptic transistors based on the combination of an InGaZnO channel and a TaO _{<i>x</i>} gate dielectric. Nanoscale, 2022, 14, 10245-10254. | 5.6 | 8 |
| 3 | Stock Price Prediction Based on an Energy-Efficient Spiking-LSTM Hardware Accelerator. Journal of Physics: Conference Series, 2021, 1828, 012050. | 0.4 | 0 |
| 4 | Performance Enhancement of Transparent Amorphous IGZO Thin-Film Transistor Realized by Sputtered Amorphous AlOx Passivation Layer. ECS Journal of Solid State Science and Technology, 2021, 10, 045006. | 1.8 | 5 |
| 5 | Design of a constant loop bandwidth phase-locked loop based on artificial neural network. IEICE Electronics Express, 2021, 18, 20210120-20210120. | 0.8 | 0 |
| 6 | Quantized STDP-based online-learning spiking neural network. Neural Computing and Applications, 2021, 33, 12317-12332. | 5.6 | 17 |
| 7 | Efficient and reconfigurable reservoir computing to realize alphabet pronunciation recognition based on processing-in-memory. Applied Physics Letters, 2021, 119, . | 3.3 | 4 |
| 8 | A Large-Size HfO2 Based RRAM Structure Suitable for Integration of One RRAM with One InGaZnO Thin Film Transistor for Large-Area Applications. ECS Journal of Solid State Science and Technology, 2021, 10, 115004. | 1.8 | 1 |
| 9 | Application of Deep Compression Technique in Spiking Neural Network Chip. IEEE Transactions on Biomedical Circuits and Systems, 2020, 14, 274-282. | 4.0 | 10 |
| 10 | Uncovering the Indium Filament Revolution in Transparent Bipolar ITO/SiO _{<i>x</i>} /ITO Resistive Switching Memories. ACS Applied Materials & Interfaces, 2020, 12, 4579-4585. | 8.0 | 17 |
| 11 | 3D Geometric Engineering of the Double Wedge-Like Electrodes for Filament-Type RRAM Device Performance Improvement. IEEE Access, 2020, 8, 4924-4934. | 4.2 | 2 |
| 12 | Investigation of Electrical Noise Signal Triggered Resistive Switching and Its Implications. IEEE Transactions on Electron Devices, 2020, 67, 4178-4184. | 3.0 | 5 |
| 13 | HfO _x -Based RRAM Device With Sandwich-Like Electrode for Thermal Budget Requirement. IEEE Transactions on Electron Devices, 2020, 67, 4193-4200. | 3.0 | 16 |
| 14 | Design of AM Self-Capacitive Transparent Touch Panel Based on a-IGZO Thin-Film Transistors. IEEE Access, 2020, 8, 76929-76934. | 4.2 | 6 |
| 15 | STBNN: Hardware-friendly spatio-temporal binary neural network with high pattern recognition accuracy. Neurocomputing, 2020, 409, 351-360. | 5.9 | 19 |
| 16 | An energy-efficient deep convolutional neural networks coprocessor for multi-object detection. Microelectronics Journal, 2020, 98, 104737. | 2.0 | 8 |
| 17 | Spikeâ€driven gated recurrent neural network processor for electrocardiogram arrhythmias detection realised in 55â€nm CMOS technology. Electronics Letters, 2020, 56, 1230-1232. | 1.0 | 7 |
| 18 | A Neuromorphic-Hardware Oriented Bio-Plausible Online-Learning Spiking Neural Network Model. IEEE Access, 2019, 7, 71730-71740. | 4.2 | 18 |

| # | Article | IF | CITATIONS |
|----|---|------|-----------|
| 19 | Uniform and electroforming-free resistive memory devices based on solution-processed triple-layered NiO/Al2O3 thin films. Applied Physics A: Materials Science and Processing, 2019, 125, 1. | 2.3 | 4 |
| 20 | Study of Recall Time of Associative Memory in a Memristive Hopfield Neural Network. IEEE Access, 2019, 7, 58876-58882. | 4.2 | 11 |
| 21 | Design of a Neural Network-Based VCO With High Linearity and Wide Tuning Range. IEEE Access, 2019, 7, 60120-60125. | 4.2 | 7 |
| 22 | Selective Scattering of Blue and Red Light Based on Silver and Gold Nanocubes. ECS Journal of Solid State Science and Technology, 2019, 8, R51-R57. | 1.8 | 2 |
| 23 | Implementation of a Low Noise Amplifier With Self-Recovery Capability. IEEE Access, 2019, 7, 43076-43083. | 4.2 | 4 |
| 24 | Surface modification of Na ₂ Ti ₃ O ₇ nanofibre arrays using N-doped graphene quantum dots as advanced anodes for sodium-ion batteries with ultra-stable and high-rate capability. Journal of Materials Chemistry A, 2019, 7, 12751-12762. | 10.3 | 83 |
| 25 | Winner-takes-all mechanism realized by memristive neural network. Applied Physics Letters, 2019, 115, . | 3.3 | 15 |
| 26 | Low energy consumption dual-ion electrochemical deionization system using NaTi2(PO4)3-AgNPs electrodes. Desalination, 2019, 451, 241-247. | 8.2 | 99 |
| 27 | Sharp selective scattering of red, green, and blue light achieved via gain material's loss compensation. Optics Express, 2019, 27, 9189. | 3.4 | 4 |
| 28 | Toward transparent projection display: recent progress in frequency-selective scattering of RGB light based on metallic nanoparticle's localized surface plasmon resonance. Opto-Electronic Advances, 2019, 2, 19002001-19002015. | 13.3 | 11 |
| 29 | Resonant scattering of green light enabled by Ag@TiO ₂ and its application in a green light projection screen. Nanoscale, 2018, 10, 2438-2446. | 5.6 | 11 |
| 30 | 3D hierarchical defect-rich NiMo3S4 nanosheet arrays grown on carbon textiles for high-performance sodium-ion batteries and hydrogen evolution reaction. Nano Energy, 2018, 49, 460-470. | 16.0 | 107 |
| 31 | Bifunctional porous iron phosphide/carbon nanostructure enabled high-performance sodium-ion battery and hydrogen evolution reaction. Energy Storage Materials, 2018, 15, 98-107. | 18.0 | 102 |
| 32 | Predicting House Price With a Memristor-Based Artificial Neural Network. IEEE Access, 2018, 6, 16523-16528. | 4.2 | 39 |
| 33 | γ-Ray Radiation Effects on an HfO ₂ -Based Resistive Memory Device. IEEE Nanotechnology Magazine, 2018, 17, 61-64. | 2.0 | 13 |
| 34 | Effect of Surface Scattering of Electrons on Ratios of Optical Absorption and Scattering to Extinction of Gold Nanoshell. Nanoscale Research Letters, 2018, 13, 299. | 5.7 | 13 |
| 35 | Realization of a Power-Efficient Transmitter Based on Integrated Artificial Neural Network. IEEE Access, 2018, 6, 68773-68781. | 4.2 | 10 |
| 36 | Smart electronic skin having gesture recognition function by LSTM neural network. Applied Physics Letters, 2018, 113, . | 3.3 | 20 |

| # | Article | IF | CITATIONS |
|----|---|------|-----------|
| 37 | Thickness effect of nickel oxide thin films on associated solution-processed write-once-read-many-times memory devices. Applied Physics A: Materials Science and Processing, 2018, 124, 1. | 2.3 | 12 |
| 38 | A Deformable and Highly Robust Ethyl Cellulose Transparent Conductor with a Scalable Silver Nanowires Bundle Micromesh. Advanced Materials, 2018, 30, e1802803. | 21.0 | 95 |
| 39 | Handwritten-Digit Recognition by Hybrid Convolutional Neural Network based on HfO2 Memristive Spiking-Neuron. Scientific Reports, 2018, 8, 12546. | 3.3 | 34 |
| 40 | Study of electrochromic characteristics in the near-infrared region of electrochromic devices based on solution-processed amorphous WO3 films. Materials Science in Semiconductor Processing, 2018, 88, 73-78. | 4.0 | 14 |
| 41 | Optical-reconfigurable carbon nanotube and indium-tin-oxide complementary thin-film transistor logic gates. Nanoscale, 2018, 10, 13122-13129. | 5.6 | 17 |
| 42 | Unlocking the potential of SnS2: Transition metal catalyzed utilization of reversible conversion and alloying reactions. Scientific Reports, 2017, 7, 41015. | 3.3 | 26 |
| 43 | Direct Observation of Indium Conductive Filaments in Transparent, Flexible, and Transferable Resistive Switching Memory. ACS Nano, 2017, 11, 1712-1718. | 14.6 | 83 |
| 44 | Modeling of a selective solar absorber thin film structure based on double TiNxOy layers for concentrated solar power applications. Solar Energy, 2017, 142, 33-38. | 6.1 | 21 |
| 45 | A MoS ₂ -based coplanar neuron transistor for logic applications. Nanotechnology, 2017, 28, 214001. | 2.6 | 12 |
| 46 | W/Cu thin film infrared reflector for TiNxOy based selective solar absorber with high thermal stability. Journal of Applied Physics, 2017, 121, . | 2.5 | 6 |
| 47 | Nanoparticle-assisted Frenkel–Poole emission in two-terminal charging-controlled memory devices based on Si-rich silicon nitride thin films. Applied Physics A: Materials Science and Processing, 2017, 123, 1. | 2.3 | 1 |
| 48 | Synthesis of IGZO ink and study of ink-jet printed IGZO thin films with different Ga concentrations. Solid-State Electronics, 2017, 138, 108-112. | 1.4 | 5 |
| 49 | Influences of water molecules on the electronic properties of atomically thin molybdenum disulfide. Applied Physics Letters, 2017, 111, . | 3.3 | 7 |
| 50 | Investigation of localized surface plasmon resonance of TiN nanoparticles in TiN_xO_y thin films. Optical Materials Express, 2016, 6, 2422. | 3.0 | 20 |
| 51 | Amorphousâ€5iâ€Based Resistive Switching Memories with Highly Reduced Electroforming Voltage and Enlarged Memory Window. Advanced Electronic Materials, 2016, 2, 1500370. | 5.1 | 23 |
| 52 | Hexagonal Boron Nitride Thin Film for Flexible Resistive Memory Applications. Advanced Functional Materials, 2016, 26, 2176-2184. | 14.9 | 167 |
| 53 | A light-stimulated synaptic transistor with synaptic plasticity and memory functions based on InGaZnOx–Al2O3 thin film structure. Journal of Applied Physics, 2016, 119, . | 2.5 | 153 |
| 54 | Design of a High Performance Selective Solar Absorber with the Structure of SiO2-TiO2-TiNxOy-Cu. ECS Journal of Solid State Science and Technology, 2016, 5, N43-N47. | 1.8 | 9 |

| # | Article | IF | CITATIONS |
|----|--|------|-----------|
| 55 | Novel concepts in functional resistive switching memories. Journal of Materials Chemistry C, 2016, 4, 9637-9645. | 5.5 | 59 |
| 56 | Direct Observation of Conducting Filaments in Tungsten Oxide Based Transparent Resistive Switching Memory. ACS Applied Materials & Interfaces, 2016, 8, 27885-27891. | 8.0 | 80 |
| 57 | Resistive Switching in p-Type Nickel Oxide/n-Type Indium Gallium Zinc Oxide Thin Film Heterojunction Structure. ECS Journal of Solid State Science and Technology, 2016, 5, Q239-Q243. | 1.8 | 5 |
| 58 | Two dimensional layered Co _{0.85} Se nanosheets as a high-capacity anode for lithium-ion batteries. Nanoscale, 2016, 8, 14992-15000. | 5.6 | 90 |
| 59 | Resistive switching characteristics of RRAM devices based on spin-coated a-IGZO thin films and ink-jet printed Ag electrodes. , 2016, , . | | 1 |
| 60 | WS ₂ –3D graphene nano-architecture networks for high performance anode materials of lithium ion batteries. RSC Advances, 2016, 6, 107768-107775. | 3.6 | 29 |
| 61 | Ultrahigh Performance of Novel Capacitive Deionization Electrodes based on A Three-Dimensional Graphene Architecture with Nanopores. Scientific Reports, 2016, 6, 18966. | 3.3 | 105 |
| 62 | 3D hierarchical Co ₃ O ₄ @Co ₃ S ₄ nanoarrays as cathode materials for asymmetric pseudocapacitors. Journal of Materials Chemistry A, 2016, 4, 3287-3296. | 10.3 | 147 |
| 63 | Hydrothermally synthesized graphene and Fe ₃ O ₄ nanocomposites for high performance capacitive deionization. RSC Advances, 2016, 6, 11967-11972. | 3.6 | 52 |
| 64 | InGaZnO Thin-Film Transistors With Coplanar Control Gates for Single-Device Logic Applications. IEEE Transactions on Electron Devices, 2016, 63, 1383-1387. | 3.0 | 8 |
| 65 | Electronic and Optical Properties of Si and Ge Nanocrystals. Advances in Materials Science and Engineering, 2016, , 215-254. | 0.4 | 0 |
| 66 | Light Emission Properties of Si Nanocrystals Embedded in a Dielectric Matrix. Advances in Materials Science and Engineering, 2016, , 255-282. | 0.4 | 0 |
| 67 | Thickness Dependence of Optical Properties of Amorphous Indium Gallium Zinc Oxide Thin Films: Effects of Free-Electrons and Quantum Confinement. ECS Solid State Letters, 2015, 4, P29-P32. | 1.4 | 11 |
| 68 | Dielectric engineering of Ge nanocrystal/SiO2 nanocomposite thin films with Ge ion implantation: Modeling and measurement. Materials and Design, 2015, 83, 713-718. | 7.0 | 9 |
| 69 | Associative memory realized by a reconfigurable memristive Hopfield neural network. Nature Communications, 2015, 6, 7522. | 12.8 | 182 |
| 70 | Evolution of the localized surface plasmon resonance and electron confinement effect with the film thickness in ultrathin Au films. Journal of Nanoparticle Research, 2015, 17, 1. | 1.9 | 6 |
| 71 | Highly spectrum-selective ultraviolet photodetector based on p-NiO/n-IGZO thin film heterojunction structure. Optics Express, 2015, 23, 27683. | 3.4 | 37 |
| 72 | Study of Multilevel High-Resistance States in HfO _{<italic>x</italic>} -Based Resistive Switching Random Access Memory by Impedance Spectroscopy. IEEE Transactions on Electron Devices, 2015, 62, 2684-2688. | 3.0 | 11 |

| # | Article | IF | CITATIONS |
|----|--|-----|-----------|
| 73 | Synaptic long-term potentiation realized in Pavlov's dog model based on a NiOx-based memristor. Journal of Applied Physics, 2014, 116, . | 2.5 | 52 |
| 74 | An Experimental Study of Lateral Charge Transfer in Silicon Nanocrystal Layer Embedded in SiO ₂ Thin Film. Nanoscience and Nanotechnology Letters, 2014, 6, 798-804. | 0.4 | 1 |
| 75 | Low dimension structures and devices for new generation photonic technology. , 2014, , . | | 0 |
| 76 | Influence of the Excess Al Content on Memory Behaviors of WORM Devices Based on Sputtered Al-Rich Aluminum Oxide Thin Films. Nanoscience and Nanotechnology Letters, 2014, 6, 845-848. | 0.4 | 0 |
| 77 | Influence of localized surface plasmon resonance and free electrons on the optical properties of ultrathin Au films: a study of the aggregation effect. Optics Express, 2014, 22, 5124. | 3.4 | 32 |
| 78 | A study on the evolution of dielectric function of ZnO thin films with decreasing film thickness. Journal of Applied Physics, 2014, 115, . | 2.5 | 27 |
| 79 | Lateral Conduction Switching in Sputtered Niâ€rich NiO Thin Films for Writeâ€Onceâ€Readâ€Manyâ€Times Memory Applications. International Journal of Applied Ceramic Technology, 2014, 11, 732-737. | 2.1 | 1 |
| 80 | Evolution of dielectric function of Al-doped ZnO thin films with thermal annealing: effect of band gap expansion and free-electron absorption. Optics Express, 2014, 22, 23086. | 3.4 | 20 |
| 81 | Tunable long-distance light transportation along Au nanoparticle chains: promising for optical interconnect. Journal of Nanoparticle Research, 2014, 16, 1. | 1.9 | 0 |
| 82 | Realization of write-once-read-many-times memory device with O ₂ plasma-treated indium gallium zinc oxide thin film. Applied Physics Letters, 2014, 104, 033505. | 3.3 | 13 |
| 83 | Al Content–Dependent Resistive Switching in Al-Rich AlO _x N _y Thin Films. Nanoscience and Nanotechnology Letters, 2014, 6, 835-839. | 0.4 | 2 |
| 84 | Review of Nanostructured Resistive Switching Memristor and Its Applications. Nanoscience and Nanotechnology Letters, 2014, 6, 729-757. | 0.4 | 76 |
| 85 | <i>A Special Issue on</i> Nanoelectronics. Nanoscience and Nanotechnology Letters, 2014, 6, 727-728. | 0.4 | 0 |
| 86 | Development of optically transparent ZnS/poly(vinylpyrrolidone) nanocomposite films with high refractive indices and high Abbe numbers. Journal of Applied Polymer Science, 2013, 129, 1793-1798. | 2.6 | 14 |
| 87 | Effect of O2 plasma immersion on electrical properties and transistor performance of indium gallium zinc oxide thin films. Thin Solid Films, 2013, 545, 533-536. | 1.8 | 19 |
| 88 | Magnetron Sputtered <scp><scp>Ni</scp></scp> â€rich Nickel Oxide Nanoâ€Films for Resistive Switching Memory Applications. International Journal of Applied Ceramic Technology, 2013, 10, 20-25. | 2.1 | 13 |
| 89 | Emulating the paired-pulse facilitation of a biological synapse with a NiOx-based memristor. Applied Physics Letters, 2013, 102, . | 3.3 | 119 |
| 90 | Electroluminescence from SiO2 Thin Film Embedded with Self-Assembled Gold Nanoparticles. Nanoscience and Nanotechnology Letters, 2013, 5, 857-860. | 0.4 | 2 |

| # | Article | IF | CITATIONS |
|-----|--|-----|-----------|
| 91 | Effects of free electrons and quantum confinement in ultrathin ZnO films: a comparison between undoped and Al-doped ZnO. Optics Express, 2013, 21, 14131. | 3.4 | 35 |
| 92 | Effect of Exposure to Ultraviolet-Activated Oxygen on the Electrical Characteristics of Amorphous Indium Gallium Zinc Oxide Thin Film Transistors. ECS Solid State Letters, 2013, 2, Q21-Q24. | 1.4 | 28 |
| 93 | Recovery from ultraviolet-induced threshold voltage shift in indium gallium zinc oxide thin film transistors by positive gate bias. Applied Physics Letters, 2013, 103, . | 3.3 | 10 |
| 94 | Design of an electronic synapse with spike time dependent plasticity based on resistive memory device. Journal of Applied Physics, 2013, 113, . | 2.5 | 14 |
| 95 | Si nanocrystal-based triple-layer anti-reflection coating for Si solar cells. Journal of Applied Physics, 2013, 114, 053109. | 2.5 | 3 |
| 96 | Ink-jet printed In-Ga-Zn oxide nonvolatile TFT memory utilizing silicon nanocrystals embedded in SiO <inf>2</inf> gate dielectric. , 2013, , . | | 1 |
| 97 | Emulating the Ebbinghaus forgetting curve of the human brain with a NiO-based memristor. Applied Physics Letters, 2013, 103, . | 3.3 | 90 |
| 98 | Temperature-Dependent Charge Transport in Al/Al Nanocrystal Embedded Al2O3 Nanocomposite/p-Si Diodes. ECS Solid State Letters, 2012, 1, Q4-Q7. | 1.4 | 11 |
| 99 | Modeling of lateral charge transfer in Si nanocrystals in SiO2 thin film. Journal of Applied Physics, 2012, 111, 073707. | 2.5 | 0 |
| 100 | Influence of SiO2 Layer on the Dielectric Function of Gold Nanoparticles on Si Substrate. Electrochemical and Solid-State Letters, 2012, 15, K5. | 2.2 | 2 |
| 101 | Realization of transient memory-loss with NiO-based resistive switching device. Applied Physics A: Materials Science and Processing, 2012, 109, 349-352. | 2.3 | 3 |
| 102 | Size-suppressed dielectrics of Ge nanocrystals: skin-deep quantum entrapment. Nanoscale, 2012, 4, 1308. | 5.6 | 7 |
| 103 | Wavelength tunable electroluminescence from randomly assembled n-CdS _x Se _{1â^'x} nanowires/p ⁺ -SiC heterojunction. Nanoscale, 2012, 4, 1467-1470. | 5.6 | 7 |
| 104 | Conduction mechanisms at low- and high-resistance states in aluminum/anodic aluminum oxide/aluminum thin film structure. Journal of Applied Physics, 2012, 112, . | 2.5 | 35 |
| 105 | Resistive Switching Behavior of Partially Anodized Aluminum Thin Film at Elevated Temperatures. IEEE Transactions on Electron Devices, 2012, 59, 2363-2367. | 3.0 | 15 |
| 106 | Controlled electroluminescence of n-ZnMgO/p-GaN light-emitting diodes. Applied Physics Letters, 2012, 101, . | 3.3 | 13 |
| 107 | Strong green emission in ZnO films after H2surface treatment. Journal Physics D: Applied Physics, 2012, 45, 185102. | 2.8 | 13 |
| 108 | A quantitative modeling of the contributions of localized surface plasmon resonance and interband transitions to absorbance of gold nanoparticles. Journal of Nanoparticle Research, 2012, 14, 1. | 1.9 | 14 |

| # | Article | IF | CITATIONS |
|-----|---|-------------------|------------------|
| 109 | Flexible Write-Once–Read-Many-Times Memory Device Based on a Nickel Oxide Thin Film. IEEE Transactions on Electron Devices, 2012, 59, 858-862. | 3.0 | 16 |
| 110 | Effect of Heat Diffusion During State Transitions in Resistive Switching Memory Device Based on Nickel-Rich Nickel Oxide Film. IEEE Transactions on Electron Devices, 2012, 59, 1558-1562. | 3.0 | 7 |
| 111 | Flexible Nanoscale Memory Device Based on Resistive Switching in Nickel Oxide Thin Film. Nanoscience and Nanotechnology Letters, 2012, 4, 940-943. | 0.4 | 4 |
| 112 | Optical Properties of Gold Nanoparticles on Heavily-Doped Si Substrate Synthesized with an Electrochemical Process. Journal of the Electrochemical Society, 2011, 158, K152. | 2.9 | 6 |
| 113 | Ultraviolet Random Lasing Action from Highly Disordered n-AlN/p-GaN Heterojunction. ACS Applied Materials & Interfaces, 2011, 3, 1726-1730. | 8.0 | 13 |
| 114 | Laterally-current-injected light-emitting diodes based on nanocrystalline-Si/SiO_2 superlattice. Optics Express, 2011, 19, 2729. | 3.4 | 17 |
| 115 | Profile Uniformity of Overlapped Oxide Dots Induced by Atomic Force Microscopy: (Journal of) Tj ETQq1 1 0.7843 Nanotechnology, 2011, 11, 899-899. | 314 rgBT / 0.9 | Overlock 10 0 |
| 116 | Bandgap expansion and dielectric suppression of self-assembled Ge nanocrystals. Journal of Applied Physics, 2011, 109, . | 2.5 | 15 |
| 117 | Annealing-Induced Changes in Electrical Characteristics of Al/Al-Rich \$hbox{Al}_{2}hbox{O}_{3}/phbox{-Si}\$ Diodes. IEEE Transactions on Electron Devices, 2011, 58, 33-38. | 3.0 | 3 |
| 118 | Two-Terminal Write-Once-Read-Many-Times Memory Device Based on Charging-Controlled Current Modulation in Al/Al-Rich \$hbox{Al}_{2}hbox{O}_{3}\$/p-Si Diode. IEEE Transactions on Electron Devices, 2011, 58, 960-965. | 3.0 | 12 |
| 119 | Influence of implantation dose on electroluminescence fromÂSi-implanted silicon nitride thin films. Applied Physics A: Materials Science and Processing, 2011, 104, 239-245. | 2.3 | 12 |
| 120 | Self-learning ability realized with a resistive switching device based on a Ni-rich nickel oxide thin film. Applied Physics A: Materials Science and Processing, 2011, 105, 855-860. | 2.3 | 9 |
| 121 | Temperature dependence of current transport in Al/Al2O3 nanocomposite thin films. Journal of Applied Physics, 2011, 110, 096108. | 2.5 | 3 |
| 122 | Competition of Resistive-Switching Mechanisms in Nickel-Rich Nickel Oxide Thin Films. Electrochemical and Solid-State Letters, 2011, 14, H400. | 2.2 | 4 |
| 123 | Temperature Dependence of Resistive Switching in Aluminum/Anodized Aluminum Film Structure. Nanoscience and Nanotechnology Letters, 2011, 3, 222-225. | 0.4 | 3 |
| 124 | Resistive Switching in a Ni-Rich Nickel Oxide Thin Film. Nanoscience and Nanotechnology Letters, 2011, 3, 267-271. | 0.4 | 1 |
| 125 | Profile Uniformity of Overlapped Oxide Dots Induced by Atomic Force Microscopy. Journal of Nanoscience and Nanotechnology, 2010, 10, 4390-4399. | 0.9 | 4 |
| 126 | A Two-Terminal Write-Once-Read-Many-Times-Memory Device Based on an Aluminum Nitride Thin Film Containing Al Nanocrystals. Journal of Nanoscience and Nanotechnology, 2010, 10, 5796-5799. | 0.9 | 4 |

| # | Article | IF | CITATIONS |
|-----|--|-----|-----------|
| 127 | Si-Based Light-Emitting Structure Synthesized with Low-Energy Ion Implantation at a Low Dosage. Journal of Nanoscience and Nanotechnology, 2010, 10, 595-598. | 0.9 | 0 |
| 128 | Charging Effect of Aluminum Nitride Thin Films Containing Al Nanocrystals. Journal of Nanoscience and Nanotechnology, 2010, 10, 599-603. | 0.9 | 6 |
| 129 | Charge Storage Behaviors of Ge Nanocrystals Embedded in SiO ₂ for the Application in Non-Volatile Memory Devices. Journal of Nanoscience and Nanotechnology, 2010, 10, 4517-4521. | 0.9 | 5 |
| 130 | Improvement of Negative Bias Temperature Instability by Stress Proximity Technique. IEEE Transactions on Electron Devices, 2010, 57, 238-243. | 3.0 | 5 |
| 131 | Electroluminescence of as-sputtered silicon-rich SiOx films. Vacuum, 2010, 84, 1043-1048. | 3.5 | 18 |
| 132 | Physics of electron mobility independent of channel orientation in n-channel transistors based on (100) silicon wafers and its experimental verification. Applied Physics Letters, 2010, 97, 133508. | 3.3 | 1 |
| 133 | Scratch properties of nickel thin films using atomic force microscopy. Journal of Vacuum Science and Technology B:Nanotechnology and Microelectronics, 2010, 28, 202-210. | 1.2 | 28 |
| 134 | Tunable Surface Plasmon Resonance of Gold Nanoparticles Self-Assembled on Fused Silica Substrate. Electrochemical and Solid-State Letters, 2010, 13, K96. | 2.2 | 10 |
| 135 | Comparison of Charge Storage Behavior of Electrons and Holes in a Continuous Ge Nanocrystal Layer. Nanoscience and Nanotechnology Letters, 2010, 2, 7-10. | 0.4 | 4 |
| 136 | Charging Effect on Conductance of Magnetron Sputtered Si Nanocrystals Embedded SiO ₂ Films. Nanoscience and Nanotechnology Letters, 2010, 2, 226-230. | 0.4 | 1 |
| 137 | The charge trapping and memory effect in SiO ₂ thin films containing Ge nanocrystals. Journal Physics D: Applied Physics, 2010, 43, 015102. | 2.8 | 10 |
| 138 | Charging effect on electroluminescence performance of nc-Si/a-SiO2 films. Journal of Applied Physics, 2010, 107, 043709. | 2.5 | 2 |
| 139 | Microstructure of Magnetron Sputtered Amorphous SiO <i>_x</i> Films: Formation of Amorphous Si Coreâ^'Shell Nanoclusters. Journal of Physical Chemistry C, 2010, 114, 2414-2420. | 3.1 | 45 |
| 140 | Collective Excitations and Dielectric Function of Self-Assembled Gold Nanoparticles on a Silicon Substrate. Electrochemical and Solid-State Letters, 2010, 13, K39. | 2.2 | 6 |
| 141 | Electroluminescence from n-In_2O_3:Sn randomly assembled nanorods/p-SiC heterojunction. Optics Express, 2010, 18, 15585. | 3.4 | 11 |
| 142 | Electrically tunable white-color electroluminescence from Si-implanted silicon nitride thin film. Optics Express, 2010, 18, 20439. | 3.4 | 28 |
| 143 | Split of surface plasmon resonance of gold nanoparticles on silicon substrate: a study of dielectric functions. Optics Express, 2010, 18, 21926. | 3.4 | 24 |
| 144 | Static dielectric constant of Al nanocrystal/Al2O3 nanocomposite thin films determined by the capacitance-voltage reconstruction technique. Applied Physics Letters, 2010, 96, 173110. | 3.3 | 6 |

| # | Article | IF | CITATIONS |
|-----|--|-----|-----------|
| 145 | Thickness effect on the band gap and optical properties of germanium thin films. Journal of Applied Physics, 2010, 107, . | 2.5 | 117 |
| 146 | Evolution of electroluminescence from multiple Si-implanted silicon nitride films with thermal annealing. Journal of Applied Physics, 2009, 105, 123101. | 2.5 | 16 |
| 147 | Parasitic memory effect induced by high erasing pulses in metal-oxide-semiconductor field-effect transistor device containing silicon nanocrystals. Journal of Applied Physics, 2009, 105, 114501. | 2.5 | 1 |
| 148 | High temperature excitonic lasing characteristics of randomly assembled SnO2 nanowires. Applied Physics Letters, 2009, 95, . | 3.3 | 16 |
| 149 | Capacitance switching in SiO2 thin film embedded with Ge nanocrystals caused by ultraviolet illumination. Applied Physics Letters, 2009, 95, 091111. | 3.3 | 1 |
| 150 | Strong violet and green-yellow electroluminescence from silicon nitride thin films multiply implanted with Si ions. Applied Physics Letters, 2009, 94, . | 3.3 | 35 |
| 151 | Anomalous capacitance-voltage characteristics of Al/Al-rich Al2O3/p-Si capacitors and their reconstruction. Applied Physics Letters, 2009, 94, 243106. | 3.3 | 4 |
| 152 | Current conduction in Al/Si nanocrystal embedded SiO2/p-Si diodes with various distributions of Si nanocrystals in the oxide. Journal of Applied Physics, 2009, 106, 013718. | 2.5 | 7 |
| 153 | Large magnetic moment obtained in Cu-doped ZnO nanoclusters. , 2009, , . | | 0 |
| 154 | Charge Storage Mechanism of Si Nanocrystals Embedded SiO ₂ Films. Nanoscience and Nanotechnology Letters, 2009, 1, 176-181. | 0.4 | 1 |
| 155 | Design of a Near-Perfect Anti Reflective Layer for Si Photodetectors Based on a SiO2Film Embedded with Si Nanocrystals. Japanese Journal of Applied Physics, 2009, 48, 060206. | 1.5 | 4 |
| 156 | Influence of thermal annealing on charge storage behaviour of Ge nanoclusters synthesized with low-energy Ge ion implantation. Journal Physics D: Applied Physics, 2009, 42, 035109. | 2.8 | 9 |
| 157 | Effect of annealing on charge transfer in Ge nanocrystal based nonvolatile memory structure. Journal of Applied Physics, 2009, 106, . | 2.5 | 24 |
| 158 | Formation of uniform nanoscale oxide layers assembled by overlapping oxide lines using atomic force microscopy. Journal of Micro/ Nanolithography, MEMS, and MOEMS, 2009, 8, 043050. | 0.9 | 6 |
| 159 | Implant Energy-Dependent Enhancement of Electroluminescence from Ge-Implanted SiO[sub 2] Thin Films. Electrochemical and Solid-State Letters, 2009, 12, H238. | 2.2 | 5 |
| 160 | Resistive switching in aluminum/anodized aluminum film structure without forming process. Journal of Applied Physics, 2009, 106, . | 2.5 | 38 |
| 161 | Charging-Induced Changes in Reverse Current–Voltage Characteristics of Al/Al-Rich \$hbox{Al}_{2}hbox{O}_{3}/hbox{p-Si}\$ Diodes. IEEE Transactions on Electron Devices, 2009, 56, 2060-2064. | 3.0 | 17 |
| 162 | Relationship Between Current Transport and Electroluminescence in \$hbox{Si}^{+}\$-Implanted \$ hbox{SiO}_{2}\$ Thin Films. IEEE Transactions on Electron Devices, 2009, 56, 2785-2791. | 3.0 | 8 |

| # | Article | IF | CITATIONS |
|-----|---|------|-----------|
| 163 | Quenching and Reactivation of Electroluminescence by Charge Trapping and Detrapping in Si-Implanted Silicon Nitride Thin Film. IEEE Transactions on Electron Devices, 2009, 56, 3212-3217. | 3.0 | 7 |
| 164 | CMOS-compatible light-emitting devices based on thin aluminum nitride film containing Al nanocrystals. Applied Physics A: Materials Science and Processing, 2009, 95, 753-756. | 2.3 | 1 |
| 165 | Evolution of Si suboxides into Si nanocrystals during rapid thermal annealing as revealed by XPS and Raman studies. Journal of Crystal Growth, 2009, 311, 1296-1301. | 1.5 | 61 |
| 166 | Optical Transmission and Photoluminescence of Silicon Nitride Thin Films Implanted with Si Ions. Electrochemical and Solid-State Letters, 2009, 12, H38. | 2.2 | 9 |
| 167 | Charging effect and capacitance modulation of Ni-rich NiO thin film. Applied Physics Letters, 2009, 95, 012104. | 3.3 | 8 |
| 168 | Charging influence on current conduction in NiO thin film embedded with Ni nanocrystals. Journal Physics D: Applied Physics, 2009, 42, 225104. | 2.8 | 1 |
| 169 | Micellar poly(styrene-b-4-vinylpyridine)-nanoparticle hybrid system for non-volatile organic transistor memory. Journal of Materials Chemistry, 2009, 19, 7354. | 6.7 | 99 |
| 170 | Magnetron Sputtered nc-Al/ <i>α</i> -Al ₂ O ₃ Nanocomposite Thin Films for Nonvolatile Memory Application. Journal of Nanoscience and Nanotechnology, 2009, 9, 4116-4120. | 0.9 | 8 |
| 171 | Influence of excess Si distribution in the gate oxide on the memory characteristics of MOSFETs. Applied Physics A: Materials Science and Processing, 2008, 91, 411-413. | 2.3 | 3 |
| 172 | Conduction switching in aluminum nitride thin films containing Al nanocrystals. Applied Physics A: Materials Science and Processing, 2008, 93, 483-487. | 2.3 | 2 |
| 173 | Nonâ€Volatile Organic Memory Applications Enabled by In Situ Synthesis of Gold Nanoparticles in a Selfâ€Assembled Block Copolymer. Advanced Materials, 2008, 20, 2325-2331. | 21.0 | 186 |
| 174 | Bottom-contact poly(3,3‴-didodecylquaterthiophene) thin-film transistors with reduced contact resistance. Organic Electronics, 2008, 9, 14-20. | 2.6 | 18 |
| 175 | Influence of oxygen partial pressure on magnetron sputtered Sr0.8Nd0.3Bi2.5Ta2O9+x ferroelectric thin films. Journal of Alloys and Compounds, 2008, 457, 549-554. | 5.5 | 18 |
| 176 | Room-Temperature Visible Electroluminescence From Aluminum Nitride Thin Film Embedded With Aluminum Nanocrystals. IEEE Transactions on Electron Devices, 2008, 55, 3605-3609. | 3.0 | 4 |
| 177 | A Simple Route to Growth of Silicon Nanowires. Journal of Nanoscience and Nanotechnology, 2008, 8, 5787-5790. | 0.9 | 3 |
| 178 | Influence of hydrogen dispersive diffusion in nitrided gate oxide on negative bias temperature instability. Applied Physics Letters, 2008, 93, 013501. | 3.3 | 3 |
| 179 | Annealing effect on the optical properties of implanted silicon in a silicon nitride matrix. Applied Physics Letters, 2008, 93, . | 3.3 | 18 |
| 180 | A comparative study on the dielectric functions of isolated Si nanocrystals and densely stacked Si nanocrystal layer embedded in SiO 2 synthesized with Si ion implantation. , 2008, , . | | 0 |

| # | Article | IF | CITATIONS |
|-----|--|-----|-----------|
| 181 | Multiferroic properties of sputtered BiFeO3 thin films. Applied Physics Letters, 2008, 92, . | 3.3 | 67 |
| 182 | Charging dynamics of discrete gold nanoparticle arrays self-assembled within a poly(styrene-b-4-vinylpyridine) diblock copolymer template. Applied Physics Letters, 2008, 93, 222908. | 3.3 | 20 |
| 183 | Ultraviolet and visible electroluminescence from n-ZnOâ^•SiOxâ^•(n,p)-Si heterostructured light-emitting diodes. Applied Physics Letters, 2008, 93, . | 3.3 | 88 |
| 184 | Charging effect of Al2O3 thin films containing Al nanocrystals. Applied Physics Letters, 2008, 93, 142106. | 3.3 | 13 |
| 185 | Light-induced instability in current conduction of aluminum nitride thin films embedded with Al nanocrystals. Applied Physics Letters, 2008, 92, 013102. | 3.3 | 6 |
| 186 | Influence of nanocrystal distribution on electroluminescence from Si ⁺ -implanted SiO 2 thin films. Proceedings of SPIE, 2008, , . | 0.8 | 0 |
| 187 | Recent Developments in Tip-Based Nanofabrication and Its Roadmap. Journal of Nanoscience and Nanotechnology, 2008, 8, 2167-2186. | 0.9 | 76 |
| 188 | Evolution of Photoluminescence Mechanisms of Si ⁺ -Implanted SiO ₂ Films with Thermal Annealing. Journal of Nanoscience and Nanotechnology, 2008, 8, 3555-3560. | 0.9 | 12 |
| 189 | CMOS-compatible light emission device based on thin aluminum nitride film containing Al nanocrystals. , 2007, , . | | 0 |
| 190 | Modeling and Characterization of Nitrogen-Enhanced Negative-Bias Temperature Instability in p-Channel MOSFETs. Journal of the Electrochemical Society, 2007, 154, G255. | 2.9 | 5 |
| 191 | Influence of charge trapping on electroluminescence from Si-nanocrystal light emitting structure. Journal of Applied Physics, 2007, 101, 104306. | 2.5 | 23 |
| 192 | APPLICATION OF SILICON NANOCRYSTAL IN NON-VOLATILE MEMORY DEVICES. , 2007, , 419-472. | | 0 |
| 193 | Measurement of Dispersion Stability of Surface-Modified Nanosized Carbon Black in Various Liquids. Journal of Nanoscience and Nanotechnology, 2007, 7, 3827-3829. | 0.9 | 3 |
| 194 | The influence of the implantation dose and energy on the electroluminescence of Si ⁺ -implanted amorphous SiO ₂ thin films. Nanotechnology, 2007, 18, 455306. | 2.6 | 19 |
| 195 | Fabrication of thin-film organic transistor on flexible substrate via ultraviolet transfer embossing. Applied Physics Letters, 2007, 90, 243502. | 3.3 | 18 |
| 196 | Photon-induced conduction modulation in SiO2 thin films embedded with Ge nanocrystals. Applied Physics Letters, 2007, 90, 103102. | 3.3 | 10 |
| 197 | Modeling and Characterization of Negative Bias Temperature Instability in p-Channel MOSFETs. ECS Transactions, 2007, 6, 283-299. | 0.5 | 2 |
| 198 | Direct Writing of Spot and Line Bonds for Microsystem Packaging Using Transmission Laser Bonding Technique. Materials and Manufacturing Processes, 2007, 22, 71-80. | 4.7 | 5 |

| # | Article | IF | CITATIONS |
|-----|---|------|-----------|
| 199 | Energy Shifts of Si Oxidation States in the System of Si Nanocrystals Embedded in SiO ₂ Matrix. Journal of Nanoscience and Nanotechnology, 2007, 7, 2506-2510. | 0.9 | 1 |
| 200 | Charging phenomena in pentacene-gold nanoparticle memory device. Applied Physics Letters, 2007, 90, 042906. | 3.3 | 141 |
| 201 | Charging effect in germanium nanocrystals embedded in a SiO2 matrix. , 2007, , . | | 0 |
| 202 | Room temperature deposition of p-type arsenic doped ZnO polycrystalline films by laser-assist filtered cathodic vacuum arc technique. Journal of Applied Physics, 2007, 101, 094905. | 2.5 | 25 |
| 203 | Charge trapping and retention behaviors of Ge nanocrystals distributed in the gate oxide near the gate synthesized by low-energy ion implantation. Journal of Applied Physics, 2007, 101, 124313. | 2.5 | 15 |
| 204 | Influence of nanocrystal size on optical properties of Si nanocrystals embedded in SiO2 synthesized by Si ion implantation. Journal of Applied Physics, 2007, 101, 103525. | 2.5 | 40 |
| 205 | Recent developments on microablation of glass materials using excimer lasers. Optics and Lasers in Engineering, 2007, 45, 975-992. | 3.8 | 41 |
| 206 | Synthesis and Electrical Transport of Novel Channel-StructuredÎ ² -AgVO3. Small, 2007, 3, 1174-1177. | 10.0 | 82 |
| 207 | Synthesis, Characterization and Oxidation Effects of Solid-State Reaction Silicon Nanocrystals. , 2006, , . | | 0 |
| 208 | Charging effect on current conduction in aluminum nitride thin films containing Al nanocrystals. Applied Physics Letters, 2006, 89, 123101. | 3.3 | 28 |
| 209 | Dielectric functions of densely stacked Si nanocrystal layer embedded in SiO2 thin films. Applied Physics Letters, 2006, 89, 251910. | 3.3 | 4 |
| 210 | A novel empirical model for NBTI recovery with the modulated measurement time frame. , 2006, , . | | 3 |
| 211 | Memory characteristics of MOSFETs with densely stacked silicon nanocrystal Layers in the gate oxide synthesized by low-energy ion beam. IEEE Electron Device Letters, 2006, 27, 231-233. | 3.9 | 47 |
| 212 | Depth Profiling of Charging Effect of Si Nanocrystals Embedded in SiO2:Â A Study of Charge Diffusion among Si Nanocrystals. Journal of Physical Chemistry B, 2006, 110, 16499-16502. | 2.6 | 12 |
| 213 | Charging mechanism in a SiO2 matrix embedded with Si nanocrystals. Journal of Applied Physics, 2006, 100, 096111. | 2.5 | 14 |
| 214 | A study of the influence of tunnel oxide thickness on the performance of flash memory based on ion-beam synthesized silicon nanocrystals. Physica Status Solidi (A) Applications and Materials Science, 2006, 203, 1291-1295. | 1.8 | 6 |
| 215 | Distinguishing the effect of crystal-field screening from the effect of valence recharging on the 2p3/2 and 3d5/2 level energies of nanostructured copper. Applied Surface Science, 2006, 252, 2101-2107. | 6.1 | 15 |
| 216 | Dielectric functions of SiO2 film embedded with silicon nanocrystals. Journal of Crystal Growth, 2006, 288, 87-91. | 1.5 | 6 |

| # | Article | IF | CITATIONS |
|-----|---|------|-----------|
| 217 | Characteristics of mechanically milled silicon nanocrystals embedded in TEOS thin films. Journal of Crystal Growth, 2006, 288, 92-95. | 1.5 | 7 |
| 218 | Silicon nanocrystal-based non-volatile memory devices. Thin Solid Films, 2006, 504, 25-27. | 1.8 | 16 |
| 219 | An electrical study of behaviors of Si nanocrystals distributed in the gate oxide near the oxide/substrate interface of a MOS structure. Thin Solid Films, 2006, 504, 32-35. | 1.8 | 0 |
| 220 | Refractive indices of textured indium tin oxide and zinc oxide thin films. Thin Solid Films, 2006, 510, 95-101. | 1.8 | 74 |
| 221 | Static dielectric constant of isolated silicon nanocrystals embedded in a SiO2 thin film. Applied Physics Letters, 2006, 88, 063103. | 3.3 | 30 |
| 222 | Influences of interface oxidation on transmission laser bonding of wafers for microsystem packaging. Microsystem Technologies, 2006, 13, 49-59. | 2.0 | 3 |
| 223 | Impact of programming mechanisms on the performance and reliability of nonvolatile memory devices based on Si nanocrystals. IEEE Transactions on Electron Devices, 2006, 53, 663-667. | 3.0 | 33 |
| 224 | Influence of Si-nanocrystal distribution in the oxide on the charging behavior of MOS structures. IEEE Transactions on Electron Devices, 2006, 53, 914-917. | 3.0 | 8 |
| 225 | Influence of Si nanocrystal distributed in the gate oxide on the MOS capacitance. IEEE Transactions on Electron Devices, 2006, 53, 730-736. | 3.0 | 13 |
| 226 | Si ion-induced instability in flatband Voltage of Si/sup +/-implanted gate oxides. IEEE Transactions on Electron Devices, 2006, 53, 1280-1282. | 3.0 | 4 |
| 227 | High-Temperature Lasing Characteristics of ZnO Epilayers. Advanced Materials, 2006, 18, 771-774. | 21.0 | 40 |
| 228 | Charge trapping phenomena of tetraethylorthosilicate thin film containing Si nanocrystals synthesized by solid-state reaction. Nanotechnology, 2006, 17, 4078-4081. | 2.6 | 3 |
| 229 | A Simple Negative Bias Temperature Instability Characterization Methodology to Minimize the Immediate Recovery Effect during Measurement. Japanese Journal of Applied Physics, 2006, 45, 6137-6140. | 1.5 | 6 |
| 230 | Dependence of barrier height and effective mass on nitrogen concentration at SiOxNy/Si interface and gate oxide thickness. Smart Materials and Structures, 2006, 15, S39-S42. | 3.5 | 12 |
| 231 | Charging/discharging of silicon nanocrystals embedded in an SiO2matrix inducing reduction/recovery in the total capacitance and tunneling current. Smart Materials and Structures, 2006, 15, S43-S46. | 3.5 | 10 |
| 232 | Analytical reaction-diffusion model and the modeling of nitrogen-enhanced negative bias temperature instability. Applied Physics Letters, 2006, 88, 172109. | 3.3 | 28 |
| 233 | Simulation of Flash Memory Characteristics based on Discrete Nanoscale Silicon. , 2006, , . | | 0 |
| 234 | Electrical characteristics of Si nanocrystal distributed in a narrow layer in the gate oxide near the gate synthesized with very-low-energy ion beams. Journal of Applied Physics, 2006, 99, 106105. | 2.5 | 9 |

| # | Article | IF | CITATIONS |
|-----|--|-----|-----------|
| 235 | Mechanism of nitrogen-enhanced negative bias temperature instability in pMOSFET. Microelectronics Reliability, 2005, 45, 19-30. | 1.7 | 34 |
| 236 | Dynamic NBTI lifetime model for inverter-like waveform. Microelectronics Reliability, 2005, 45, 1115-1118. | 1.7 | 7 |
| 237 | Effects of annealing on the microstructure and electrical properties of TaN-Cu nanocomposite thin films. Surface and Coatings Technology, 2005, 193, 173-177. | 4.8 | 17 |
| 238 | Fabrication of n-ZnO:Alâ^•p-SiC(4H) heterojunction light-emitting diodes by filtered cathodic vacuum arc technique. Applied Physics Letters, 2005, 86, 241111. | 3.3 | 97 |
| 239 | Impact of Nonuniform Graded Dopant Profile in Polysilicon Gate on Gate Leakage Current. IEEE Transactions on Electron Devices, 2005, 52, 1200-1204. | 3.0 | 1 |
| 240 | Characterization of Si Nanocrystals Embedded in SiO ₂ with X-Ray Photoelectron Spectroscopy. Journal of Metastable and Nanocrystalline Materials, 2005, 23, 11-14. | 0.1 | 0 |
| 241 | Optical-Property Profiling of SiO ₂ Films Containing Si Nanocrystals Formed by Si ⁺ Implantation. Journal of Metastable and Nanocrystalline Materials, 2005, 23, 133-136. | 0.1 | 0 |
| 242 | Modulation of Capacitance Magnitude by Charging/Discharging in Silicon Nanocrystals Distributed Throughout the Gate Oxide in MOS Structures. Electrochemical and Solid-State Letters, 2005, 8, G8. | 2.2 | 8 |
| 243 | Random capacitance modulation due to charging/discharging in Si nanocrystals embedded in gate dielectric. Nanotechnology, 2005, 16, 1119-1122. | 2.6 | 6 |
| 244 | An approach to optical-property profiling of a planar-waveguide structure of Si nanocrystals embedded in SiO2. Nanotechnology, 2005, 16, 2657-2660. | 2.6 | 2 |
| 245 | Memory effect of Al-rich AlN films synthesized with rf magnetron sputtering. Applied Physics Letters, 2005, 87, 033112. | 3.3 | 26 |
| 246 | Thermal annealing effect on the band gap and dielectric functions of silicon nanocrystals embedded in SiO2 matrix. Applied Physics Letters, 2005, 87, 121903. | 3.3 | 25 |
| 247 | Influence of silicon-nanocrystal distribution in SiO2 matrix on charge injection and charge decay. Applied Physics Letters, 2005, 86, 152110. | 3.3 | 18 |
| 248 | Defect-induced photoluminescence from tetraethylorthosilicate thin films containing mechanically milled silicon nanocrystals. Journal of Applied Physics, 2005, 97, 104307. | 2.5 | 15 |
| 249 | Nanofabrication by scanning probe microscope lithography: A review. Journal of Vacuum Science & Technology an Official Journal of the American Vacuum Society B, Microelectronics Processing and Phenomena, 2005, 23, 877. | 1.6 | 404 |
| 250 | DISSIPATION OF CHARGES IN SILICON NANOCRYSTALS EMBEDDED IN SIO2 DIELECTRIC FILMS: AN ELECTROSTATIC FORCE MICROSCOPY STUDY. International Journal of Nanoscience, 2005, 04, 709-715. | 0.7 | 0 |
| 251 | Optical properties of silicon nanocrystals embedded in aSiO2matrix. Physical Review B, 2005, 72, . | 3.2 | 99 |
| 252 | A quantitative study of the relationship between the oxide charge trapping over the drain extension and the off-state drain leakage current. Applied Physics Letters, 2004, 85, 4211-4213. | 3.3 | 3 |

| # | Article | IF | CITATIONS |
|-----|---|-----|-----------|
| 253 | Influence of nitrogen on tunneling barrier heights and effective masses of electrons and holes at lightly-nitrided SiO2â^•Si interface. Journal of Applied Physics, 2004, 96, 5912-5914. | 2.5 | 17 |
| 254 | Profile of optical constants of SiO2 thin films containing Si nanocrystals. Journal of Applied Physics, 2004, 95, 8481-8483. | 2.5 | 9 |
| 255 | Visualizing charge transport in silicon nanocrystals embedded in SiO2 films with electrostatic force microscopy. Applied Physics Letters, 2004, 85, 2941-2943. | 3.3 | 45 |
| 256 | Charging Effect on Electrical Characteristics of MOS Structures with Si Nanocrystal Distribution in Gate Oxide. Electrochemical and Solid-State Letters, 2004, 7, G134. | 2.2 | 26 |
| 257 | Dielectric suppression of nanosolid silicon. Nanotechnology, 2004, 15, 1802-1806. | 2.6 | 40 |
| 258 | Core-Level Shift of Si Nanocrystals Embedded in a SiO2Matrix. Journal of Physical Chemistry B, 2004, 108, 16609-16612. | 2.6 | 30 |
| 259 | Electrical properties of TaN–Cu nanocomposite thin films. Ceramics International, 2004, 30, 1879-1883. | 4.8 | 28 |
| 260 | Atomic Modeling of Nitrogen Neighboring Effect on Negative Bias Temperature Instability of pMOSFETs. IEEE Electron Device Letters, 2004, 25, 504-506. | 3.9 | 20 |
| 261 | Real time evolution of charge decay characteristics in silicon nanocrystals. , 2004, , . | | Ο |
| 262 | Length, Strength, Extensibility, and Thermal Stability of a Auâ^'Au Bond in the Gold Monatomic Chain. Journal of Physical Chemistry B, 2004, 108, 2162-2167. | 2.6 | 37 |
| 263 | Dependence of barrier height and effective electron mass on gate oxide thickness and nitrogen concentration at SiO x N y /Si interface. , 2004, 5274, 493. | | 0 |
| 264 | Evolutions and distributions of Si nanocrystals and other Si oxidation states in Si-implanted SiO2 films. , 2004, 5275, 374. | | 0 |
| 265 | Optical properties and their depth profiling of Si nanocrystals embedded in SiO 2 matrix. , 2004, 5275, 378. | | 0 |
| 266 | Charging/discharging induced premature breakdown/recovery in Si nanocrystals embedded in SiO 2 matrix. , 2004, 5275, 18. | | 0 |
| 267 | Gate oxide thickness dependence of edge charge trapping in nmos transistors caused by charge injection under constant-current stress. IEEE Transactions on Electron Devices, 2003, 50, 1548-1550. | 3.0 | 5 |
| 268 | Photoluminescence of Si Nanosolids Near the Lower End of the Size Limit ChemInform, 2003, 34, no. | 0.0 | 0 |
| 269 | Nitrogen-enhanced negative bias temperature instability: An insight by experiment and first-principle calculations. Applied Physics Letters, 2003, 82, 1881-1883. | 3.3 | 66 |
| 270 | Discriminating Crystal Binding from the Atomic Trapping of a Core Electron at Energy Levels Shifted by Surface Relaxation or Nanosolid Formation. Journal of Physical Chemistry B, 2003, 107, 411-414. | 2.6 | 25 |

| # | Article | IF | CITATIONS |
|-----|--|-----|-----------|
| 271 | A study on Si nanocrystal formation in Si-implanted SiO2films by x-ray photoelectron spectroscopy. Journal Physics D: Applied Physics, 2003, 36, L97-L100. | 2.8 | 66 |
| 272 | Relationship between interfacial nitrogen concentration and activation energies of fixed-charge trapping and interface state generation under bias-temperature stress condition. Applied Physics Letters, 2003, 82, 269-271. | 3.3 | 39 |
| 273 | Dielectric functions of Si nanocrystals embedded in aSiO2matrix. Physical Review B, 2003, 68, . | 3.2 | 49 |
| 274 | Influences of nitridation on tunneling barrier change and charge trapping caused by electrical stress. Journal of Applied Physics, 2003, 93, 3114-3116. | 2.5 | 1 |
| 275 | Study of negative-bias temperature-instability-induced defects using first-principle approach. Applied Physics Letters, 2003, 83, 3063-3065. | 3.3 | 9 |
| 276 | Linear relationship between H+-trapping reaction energy and defect generation: Insight into nitrogen-enhanced negative bias temperature instability. Applied Physics Letters, 2003, 83, 530-532. | 3.3 | 22 |
| 277 | Influence of interfacial nitrogen on edge charge trapping at the interface of gate oxide/drain extension in metal–oxideà€"semiconductor transistors. Applied Physics Letters, 2003, 82, 3113-3115. | 3.3 | 4 |
| 278 | Depth Profiling of Si Oxidation States in Si-Implanted SiO2Films by X-Ray Photoelectron Spectroscopy. Japanese Journal of Applied Physics, 2003, 42, L1394-L1396. | 1.5 | 7 |
| 279 | Charging effect of Si nanocrystals in gate oxide near gate on MOS capacitance. Electronics Letters, 2003, 39, 1164. | 1.0 | 6 |
| 280 | Depth profiling of Si nanocrystals in Si-implanted SiO2 films by spectroscopic ellipsometry. Applied Physics Letters, 2002, 81, 4724-4726. | 3.3 | 18 |
| 281 | Post-Breakdown Conduction Instability of Ultrathin SiO2Films Observed in Ramped-Current and Ramped-Voltage Current–Voltage Measurements. Japanese Journal of Applied Physics, 2002, 41, 3047-3051. | 1.5 | 5 |
| 282 | Influence of nitrogen concentration in nitrided oxides on interface trap generation caused by Fowler-Nordheim injection. Journal Physics D: Applied Physics, 2002, 35, L115-L117. | 2.8 | 1 |
| 283 | Influences of Nitridation on Barrier Height Change Caused by Electrical Stress. Japanese Journal of Applied Physics, 2002, 41, L1425-L1427. | 1.5 | 0 |
| 284 | Power-Law Dependence of Charge Trapping on Injected Charge in Very Thin SiO2 Films. Japanese Journal of Applied Physics, 2002, 41, L384-L386. | 1.5 | 2 |
| 285 | Influence of Nitrogen Proximity from the Si/SiO2 Interface on Negative Bias Temperature Instability. Japanese Journal of Applied Physics, 2002, 41, L1031-L1033. | 1.5 | 12 |
| 286 | Suppression of Nitridation-Induced Interface Traps and Hole Mobility Degradation by Nitrogen Plasma Nitridation. Electrochemical and Solid-State Letters, 2002, 5, G26. | 2.2 | 3 |
| 287 | Barrier Height Change in Very Thin SiO[sub 2] Films Caused by Charge Injection. Electrochemical and Solid-State Letters, 2002, 5, G96. | 2.2 | 2 |
| 288 | Photoluminescence of Si Nanosolids near the Lower End of the Size Limit. Journal of Physical Chemistry B, 2002, 106, 11725-11727. | 2.6 | 43 |

| # | Article | IF | CITATIONS |
|-----|--|-----|-----------|
| 289 | Negative Bias Temperature Instability on Plasma-Nitrided Silicon Dioxide Film. Japanese Journal of Applied Physics, 2002, 41, L314-L316. | 1.5 | 25 |
| 290 | A simple technique to determine barrier height change in gate oxide caused by electrical stress. IEEE Transactions on Electron Devices, 2002, 49, 1493-1496. | 3.0 | 54 |
| 291 | Upper limit of blue shift in the photoluminescence of CdSe and CdS nanosolids. Acta Materialia, 2002, 50, 4687-4693. | 7.9 | 43 |
| 292 | A novel approach to quantitative determination of charge trapping near channel/drain edge in MOSFETs. Solid-State Electronics, 2002, 46, 2013-2016. | 1.4 | 6 |
| 293 | Characterization of interface degradation in deep submicron MOSFETs by gate-controlled-diode measurement. Microelectronics Journal, 2002, 33, 639-643. | 2.0 | 2 |
| 294 | Bond-orderÂbond-lengthÂbond-strength (bond-OLS) correlation mechanism for the shape-and-size dependence of a nanosolid. Journal of Physics Condensed Matter, 2002, 14, 7781-7795. | 1.8 | 125 |
| 295 | Snapback behaviour and its similarity to the switching behaviour in ultra-thin silicon dioxide films after hard breakdown. Journal Physics D: Applied Physics, 2001, 34, L95-L98. | 2.8 | 11 |
| 296 | An extended `quantum confinement' theory: surface-coordination imperfection modifies the entire band structure of a nanosolid. Journal Physics D: Applied Physics, 2001, 34, 3470-3479. | 2.8 | 82 |
| 297 | On the switching behaviour of post-breakdown conduction in ultra-thin SiO2films. Semiconductor Science and Technology, 2001, 16, 793-797. | 2.0 | 10 |
| 298 | Snapback behavior of the postbreakdown l–V characteristics in ultrathin SiO2 films. Applied Physics Letters, 2001, 78, 492-494. | 3.3 | 23 |
| 299 | Modeling the Post-Breakdown I-V Characteristics of Ultrathin SiO2 Films with Multiple Snapbacks. Japanese Journal of Applied Physics, 2001, 40, L666-L668. | 1.5 | 3 |
| 300 | Frequency-controlled low-level current source based on charge pumping. Electronics Letters, 2001, 37, 1046. | 1.0 | 4 |
| 301 | Reproducibility of transmission line measurement of bipolar I-V characteristics of MOSFETs. IEEE Transactions on Instrumentation and Measurement, 1999, 48, 721-723. | 4.7 | 4 |
| 302 | Interface trap generation by FN injection under dynamic oxide field stress. IEEE Transactions on Electron Devices, 1998, 45, 1920-1926. | 3.0 | 32 |
| 303 | Post-stress interface trap generation induced by oxide-field stress with FN injection. IEEE Transactions on Electron Devices, 1998, 45, 1972-1977. | 3.0 | 10 |
| 304 | Influence of voltage contacts on precision measurements of the quantized Hall resistance: an effect of externally injected current. IEEE Transactions on Instrumentation and Measurement, 1998, 47, 592-594. | 4.7 | 1 |
| 305 | Electrically induced room temperature metastability in semi-insulating GaAs. Solid State Communications, 1998, 108, 907-911. | 1.9 | 2 |
| 306 | Instabilities in gate-controlled-diode characteristics of n-MOSFETs following hot-carrier injection. Semiconductor Science and Technology, 1997, 12, 1365-1368. | 2.0 | 0 |

| # | Article | IF | CITATIONS |
|-----|---|-----|-----------|
| 307 | Reverse l–V characteristics of Au/semi-insulating GaAs(1 0 0). Solid State Communications, 1997, 101, 715-720. | 1.9 | 14 |
| 308 | Fermi level position at metal/semi-insulating-GaAs (1 0 0) interfaces studied by photoelectric techniques. Solid State Communications, 1997, 102, 833-836. | 1.9 | 2 |
| 309 | Optical transitions in germanium dioxide. Thin Solid Films, 1996, 283, 230-234. | 1.8 | 6 |
| 310 | Determination of substrate doping, substrate carrier lifetime and density of surface recombination centres of MOSFETs by gate-controlled-diode measurements. Semiconductor Science and Technology, 1996, 11, 672-678. | 2.0 | 8 |
| 311 | Temperature dependence of the ideality factor of GaAs and Si schottky diodes. Physica Status Solidi A, 1995, 152, 563-571. | 1.7 | 25 |
| 312 | Optical Properties of Interband Transitions in the Oxygenâ€Plasmaâ€Anodised Film on Gallium Arsenide ã€^100〉. Physica Status Solidi (B): Basic Research, 1995, 192, 217-222. | 1.5 | 0 |
| 313 | Numerical study of electrostatic properties of metal/semi-insulating GaAs contacts. Solid State Communications, 1995, 94, 287-291. | 1.9 | 2 |
| 314 | Cathodoluminescence from interband transitions in germanium (111) and gallium arsenide (100) crystals. Physical Review B, 1995, 52, 1452-1455. | 3.2 | 1 |
| 315 | Interfacial Fermi level and surface band bending in Ni/semiâ€insulating GaAs contact. Journal of Applied Physics, 1995, 78, 4796-4798. | 2.5 | 5 |
| 316 | Influence of annealing on Fermiâ€level pinning and current transport at Auâ€ 6 i and Auâ€GaAs Interfaces. Journal of Applied Physics, 1995, 77, 6724-6726. | 2.5 | 4 |
| 317 | Determination of leakage resistance of Schottky contacts by photovoltage measurements. Journal of Applied Physics, 1994, 75, 7361-7364. | 2.5 | 4 |
| 318 | Numerical modeling of transient characteristics of photovoltage in Schottky contacts. Journal of Applied Physics, 1994, 76, 7624-7626. | 2.5 | 0 |
| 319 | Leakage current induced drop in Ef in pes studies of Schottky barrier formation. Solid State Communications, 1994, 89, 779-781. | 1.9 | 1 |
| 320 | A study of recombination current in Schottky contacts by photovoltage measurements. Semiconductor Science and Technology, 1994, 9, 2101-2106. | 2.0 | 6 |
| 321 | Characterization of Ptâ€Si interface by spectroscopic ellipsometry. Journal of Applied Physics, 1994, 76, 7423-7427. | 2.5 | 3 |
| 322 | Numerical study of the decay of photovoltage at metal-semiconductor interfaces. Solid State Communications, 1993, 87, 1163-1167. | 1.9 | 1 |
| 323 | Current transport and its effect on the determination of the Schottky-barrier height in a typical system: Gold on silicon. Solid-State Electronics, 1993, 36, 949-954. | 1.4 | 31 |
| 324 | A calculation of the photovoltage at the metal-semiconductor interface. Surface Science, 1993, 294, 367-372. | 1.9 | 5 |

| # | Article | IF | CITATIONS |
|-----|---|-----|-----------|
| 325 | Reverse I-V characteristics of Au/semi-insulating InP (100). Semiconductor Science and Technology, 1993, 8, 709-711. | 2.0 | 8 |
| 326 | A photovoltaic study of current transport and its influence on the determination of the Schottky barrier height in Schottky diodes. Semiconductor Science and Technology, 1993, 8, 2085-2091. | 2.0 | 12 |
| 327 | The effect of the temperature dependence of the ideality factor on metal-semiconductor solar devices. Semiconductor Science and Technology, 1993, 8, 1357-1360. | 2.0 | 12 |
| 328 | Investigation of Schottky barrier formation for transition metal overlayers on InP and GaP(110) surfaces. Surface Science, 1992, 269-270, 979-987. | 1.9 | 11 |
| 329 | Theoretical study of leakage current effect on surface photovoltage induced by photoemission. Solid State Communications, 1992, 84, 815-818. | 1.9 | 8 |
| 330 | The interaction of platinum with GaP(110): band bending and surface photovoltage effects. Applied Surface Science, 1992, 56-58, 233-241. | 6.1 | 18 |
| 331 | Interface chemistry and band bending induced by Pt deposition onto GaP(110). Surface Science, 1991, 251-252, 472-477. | 1.9 | 19 |
| 332 | Improvements in the PSB AC-DC transfer capabilities and a proposal for range extension. , 0, , . | | 3 |
| 333 | Instability in post-breakdown conduction in ultra-thin gate oxide. , 0, , . | | 0 |
| 334 | Influence of trapped charges on low-level leakage current in thin silicon dioxide films. , 0, , . | | 1 |
| 335 | Study of edge charge trapping in gate oxide caused by FN and hot-carrier injection. , 0, , . | | 0 |
| 336 | Study of influence of nitrogen concentration in nitrided oxide on interface trap generation. , 0, , . | | 0 |
| 337 | Effects of post-decoupled-plasma-nitridation annealing of ultra-thin gate oxide. , 0, , . | | 0 |
| 338 | Characterization of ultrathin plasma nitrided gate dielectrics in pMOSFET for 0.18 \hat{l} $\!$ | | 1 |
| 339 | Negative-bias-temperature-instability (NBTI) for p/sup +/-gate pMOSFET with ultra-thin plasma-nitrided gate dielectrics. , 0, , . | | 2 |
| 340 | A new waveform-dependent lifetime model for dynamic NBTI in PMOS transistor. , 0, , . | | 4 |
| 341 | New Structures and Materials for Next Generation Photonic Technology. Applied Mechanics and Materials, 0, 120, 556-560. | 0.2 | 0 |
| | | | |